JOURNAL OF MATERIALS SCIENCE 28 (1993) 4068–4072

Morphology and rotation twin in ZnSe on GaAs (111)

M. FUJII
Nagasaki Institute of Applied Science, Nagasaki 851-01, Japan
H. IWANAGA, N. SHIBATA
Faculty of Liberal Arts, Nagasaki University, Nagasaki 852, Japan
H. OGAWA, M. NISHIO
Department of Electrical Engineering, Saga University, Saga 840, Japan

ZnSe crystals were grown by a vapour transport method on a GaAs substrate with a (1 1 1) A or ($\bar{1}\,\bar{1}\,\bar{1}$) B surface. Crystals obtained on the (1 1 1) A surface of the substrate were fine crystals and hexagonal plates. Whereas crystals grown on the ($\bar{1}\,\bar{1}\,\bar{1}$) B were uniform thin films on which trigonal hills and trigonal pyramids developed. These crystallites had a complicated morphology. In addition, the hill and pyramid grown on the ($\bar{1}\,\bar{1}\,\bar{1}$) B surface contained rotation twins around a polar axis parallel to the growth direction or around the other polar axes.

1. Introduction

ZnSe crystals have been studied as a possible material for blue-light emitting devices. Epitaxial growth of ZnSe on GaAs substrates has been carried out by molecular-beam epitaxy (MBE) [1, 2], metal–organic chemical vapour deposition (MOCVD) [3–5] and atomic-layer epitaxy (ALE) [6] to reduce intrinsic point defects and residual impurities. Kitagawa *et al.* [7] reported the morphology and the difference in the growth velocity of the ZnSe crystals grown on the (1 1 1) A, ($\bar{1}\,\bar{1}\,\bar{1}$) B and (1 0 0) planes of the GaAs substrates by the vapour phase method.

In a previous paper [8], three morphological features of ZnSe crystals growing from Se and/or As solvents were reported. This paper describes the morphology of various types of ZnSe crystals epitaxially grown on the GaAs substrates by the vapour transport method and the rotation twin found in the crystal.

2. Experimental procedure

Fig. 1 illustrates the apparatus used for epitaxial growth of ZnSe by the vapour transport method. The reaction quartz tube is 32 mm in diameter and 520 mm in length. High purity Ar gas flows into the quartz tube through its entrance (main flow) and also through the bypass tube (bypass flow). The bypass flow had the same direction as that of the main flow and its outlet is usually placed beyond the ZnSe source in the main flow. The main and bypass flows were controlled accurately by a mass-flow controller. A charge of approximately 30 g of ZnSe polycrystals was placed in a quartz boat. ZnSe single crystals were grown on the (1 1 1) A and ($\bar{1}\,\bar{1}\,\bar{1}$) B planes of the GaAs substrates set on the quartz plate.

The ZnSe sources and the GaAs substrates were treated by the following procedures before they were set in the reaction quartz tube. ZnSe polycrystals for optical purposes were cut into a suitable size by an ultrasonic cutter. After being degreased with organic solvent and rinsed with deionized water, they were chemically polished in a solution of about 20 mol % NaOH at about 100 °C and rinsed again with deionized water. Commercial GaAs crystals with a mirror-like surface were cleaved into a size of 8×8 mm to use as the substrates. Similarly to the ZnSe sources, after being degreased with organic solvent and rinsed with deionized water the GaAs crystals were slightly chemically polished in a solution of $3H_2SO_4 + H_2O_2 + H_2O$ at about 40 °C and rinsed with deionized water.

The reaction quartz tube was placed in a three-zone resistance-heating furnace. During the growth, ZnSe polycrystals were kept at 980 °C and the temperatures of the GaAs (1 1 1) A and ($\bar{1}\,\bar{1}\,\bar{1}$) B planes were 830 °C and 770 °C, respectively.

Morphological studies of ZnSe crystals were carried out by scanning electron microscopy (SEM) and optical microscopy. Furthermore, characteristic X-ray images of Se and Ga on the cross-section of the crystal were taken by electron-probe micro-analysis (EPMA).

3. Results and discussion

The morphology of the epitaxially grown crystal obtained on the GaAs (1 1 1) A surface differed from that on the ($\bar{1}\,\bar{1}\,\bar{1}$) B surface. These crystals were confirmed

0022–2461

to be ZnSe crystals by the X-ray Debye–Scherrer method.

3.1. ZnSe crystals on GaAs (1 1 1) A substrate

Fig. 2 shows a top view of ZnSe crystals grown on the GaAs (1 1 1) A substrate. Fine crystals and hexagonal plates are seen. These plates seem to be epitaxially grown on the substrate, because their top surface is parallel to the (1 1 1) substrate face and the corresponding edges of each plate are parallel.

Fig. 3 shows SEM micrographs of ZnSe crystals; hexagonal plates, fine crystals and hexagonal pyramids with sharp or flat tops are observed. A plate, P, in Fig. 3a shows layer growth as well as overgrowth, i.e. upper layers hang out over lower ones. The arrow in Fig. 3b indicates the joining of the two plates Q and R. Their top surface is a flat (1 1 1), but a slight depression is seen where they join. The top surface of the table-like crystal in Fig. 3c should be the (1 1 1) A, and there is a space between two legs of the table under the top plate, where many fine crystals are found. The table-like crystal is composed of two overgrowing plates which are the same height.

3.2. ZnSe crystals on GaAs ($\bar{1}\,\bar{1}\,\bar{1}$) B substrate

ZnSe trigonal hills are observed on the GaAs ($\bar{1}\,\bar{1}\,\bar{1}$) B substrate (Fig. 4). It is clear that the hills are epitaxially grown on the substrate, because all of them have the same orientation.

3.2.1. Morphology of trigonal hills

Analytical studies were carried out on ZnSe by EPMA, as well as morphological studies by SEM.

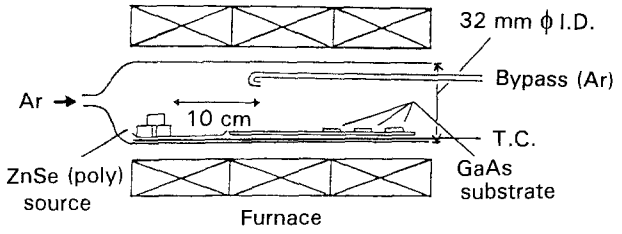

Figure 1 Schematic drawing of the apparatus for epitaxial growth.

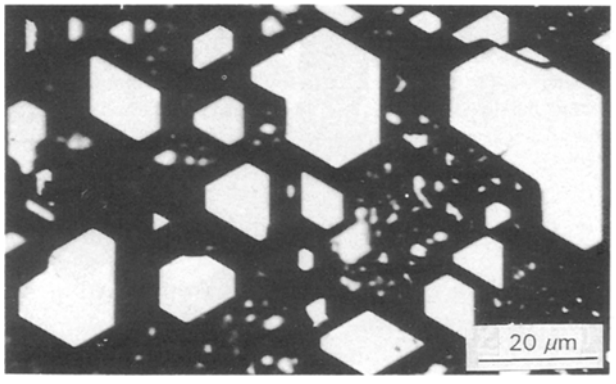

Figure 2 An optical micrograph of ZnSe crystals obtained on the (1 1 1) A surface of the GaAs substrate.

Fig. 5a and b show SEM micrographs of a cross-section cleaved along the line AD in Fig. 4. Growth of a thin film on the GaAs substrate can be clearly recognized (X and Y in Fig. 5b), on which a trigonal hill of ZnSe is grown. Fig. 5c and d are characteristic X-ray images of Se and Ga, taken by EPMA, on the cross-section in Fig. 5b. The bright images in Fig. 5c

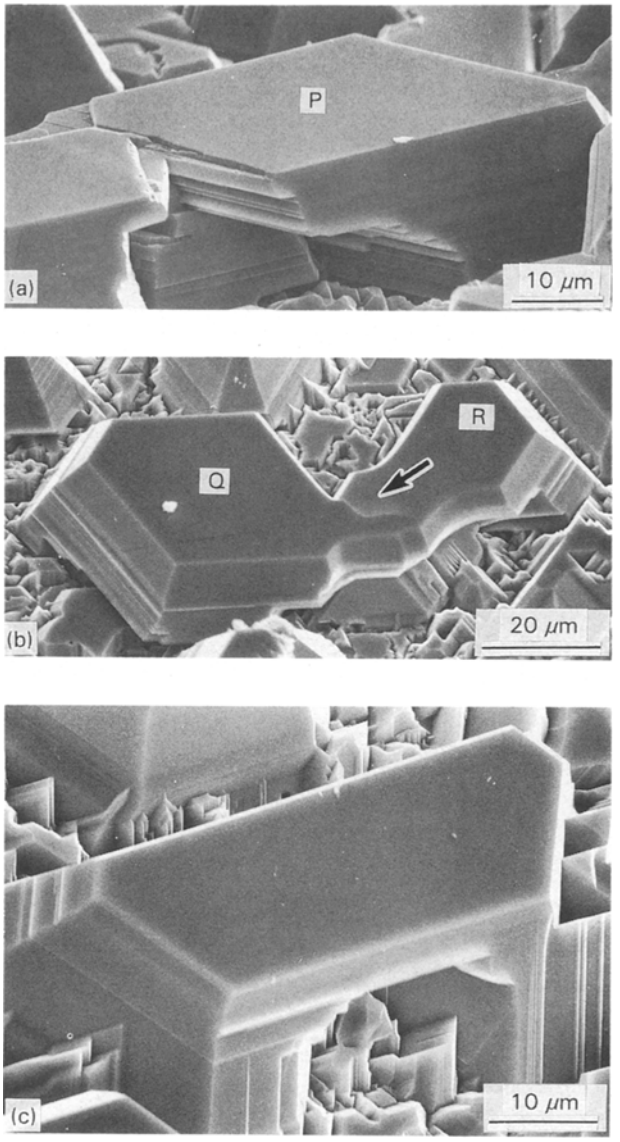

Figure 3 Hexagonal plates and fine crystals; (a) layer growth and overgrowth are seen, (b) joining of two hexagonal plates, and (c) an example of table-like crystals.

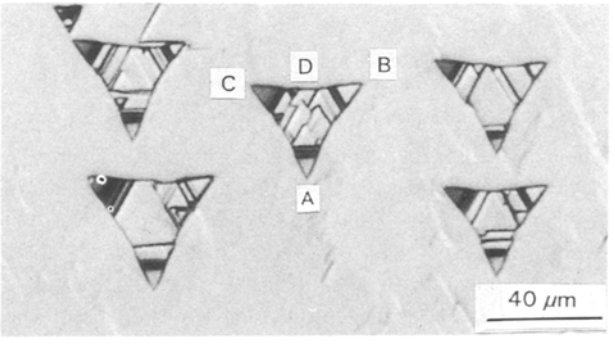

Figure 4 ZnSe thin film and trigonal hills obtained on the ($\bar{1}\,\bar{1}\,\bar{1}$) B surface of the substrate.

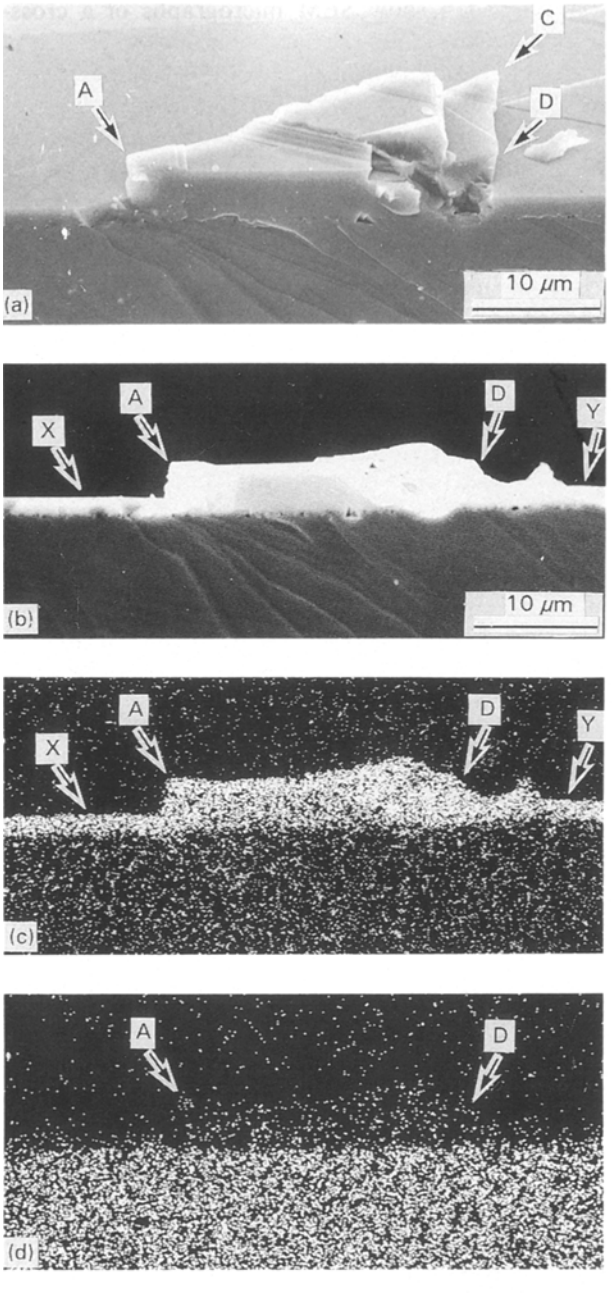

Figure 5 (a) and (b) scanning electron micrographs of a cross-section of the substrate; the thin film and the trigonal hill are cleaved along the line AD in Fig. 4. (c) and (d) characteristic X-ray images of Se and Ga on the cross-section in (b) taken by EPMA.

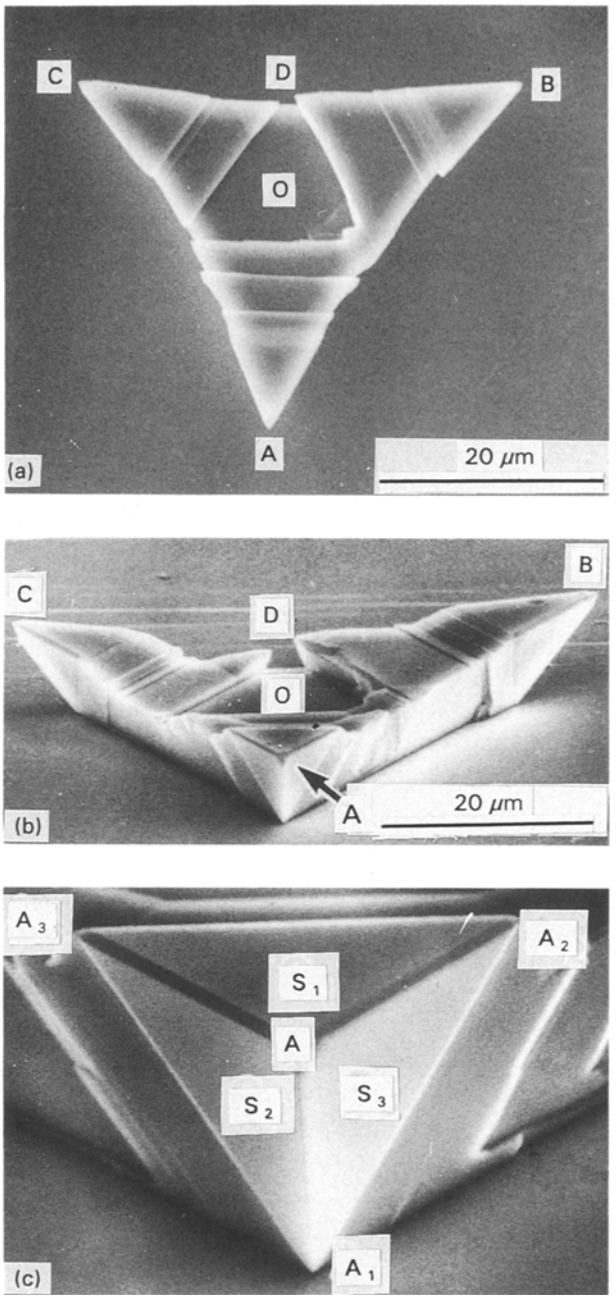

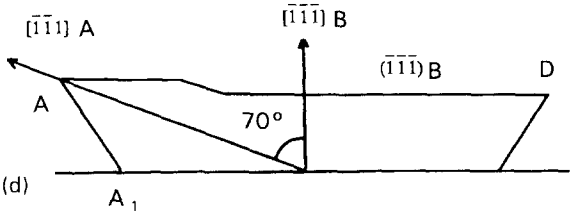

Figure 6 A scanning electron micrograph of a ZnSe trigonal hill: (a) viewing the $[\bar{1}\,\bar{1}\,\bar{1}]$ B plane vertically; (b) after a rotation by 70° around the side BC of the hill; (c) an enlarged photograph of A in (b); and (d) a schematic drawing of a cross-section of the trigonal hill.

and d are due to Se atoms in the thin ZnSe film and Ga atoms in the GaAs substrate, respectively. It is clear from Fig. 5a–d that first a thin ZnSe film of 2 μm in thickness is grown uniformly on the substrate and then the ZnSe trigonal hill of 5 μm in thickness is grown.

Fig. 6a–c are SEM micrographs of a ZnSe trigonal hill. Fig. 6a is a top view of the hill, and Fig. 6b is a view after a rotation of 70° around the side BC in Fig. 6a; that is, a view observed along the $[\bar{1}\,\bar{1}\,1]$ direction. A cluster of fine steps parallel to the $\langle 1\,\bar{1}\,0\rangle$ is found near the tips A, B and C. These steps were developed by trapping molecules supplied from the tip. Due to the preferential growth at the tip, the corner of the hill is slightly higher than the centre (O in the figure) and the side of the hill (AB, BC and CA in Fig. 6a) is not strictly straight but a little bent in the middle.

Fig. 6c is a close-up view of the tip A in Fig. 6b along the same orientation. Three edges AA_1, AA_2 and AA_3, and also three facets S_1, S_2 and S_3, have a three-fold symmetry around an axis passing the point A. These facts imply that the facets S_1, S_2 and S_3 are three planes composing a regular tetrahedron of the

zincblende structure. Moreover, the facet S_1 is a Se atom plane of the $\{1\,1\,1\}$ type, since it is parallel to the substrate face. All of the facets are the $\{\bar{1}\,\bar{1}\,\bar{1}\}$ B plane, because four planes of the regular tetrahedron should have the same polarity in the zincblende structure.

A cross-sectional view of the trigonal hill, cut along the line AD in Fig. 6a and perpendicular to the substrate surface, is schematically illustrated in Fig. 6d. The growth direction of the flat plane of the hill (O in Fig. 6a) is the $[\bar{1}\,\bar{1}\,\bar{1}]$ B, while that of the tip is the $[\bar{1}\,\bar{1}\,1]$ A. The growth of the trigonal hill is attributed to the fact that the growth velocity along the $[1\,1\,1]$ A is faster than that along the $[\bar{1}\,\bar{1}\,\bar{1}]$ B.

Very similar trigonal hills of ZnSe have been reported by Kitagawa *et al.* [7], though they have a small flat $\{1\,1\,1\}$ A plane at each corner, differing from the hills here whose corner has a pointed tip. It is likely that Kitagawa's hills are formed by the layer growth of the $\{\bar{1}\,\bar{1}\,1\}$ A plane, whereas ours are mainly due to the step development on the $\{\bar{1}\,\bar{1}\,\bar{1}\}$ B plane by deposition of molecules migrating from the tip of the hill corner. A smaller growth rate of the $\{\bar{1}\,\bar{1}\,\bar{1}\}$ B than of the $\{1\,1\,1\}$ A is common in both the authors' and Kitagawa's hills.

3.2.2. Rotation-twinned trigonal hills and projections

The trigonal hill of ZnSe is sometimes oppositely oriented to the usual orientation, as shown in Fig. 7. In Fig. 7 a hill S can be obtained by rotating the usual hill by 60° or 180° around an axis perpendicular to the substrate; that is, an axis parallel to the polar direction. This suggests that the hill S has a rotation-twin relation to the other hills. Rotation twins have been reported around the polar axis found in ZnSe [9] and CdTe crystals [10] grown by the Bridgman method, and also in GaP whiskers [11] formed by a closed-tube method.

In addition, one or more projections are observed to grow from the side of a trigonal hill which is coherent to the substrate. Fig. 8 shows a trigonal hill, S_0, with a projection S_1. From its orientation, this projection is found to be in a rotation-twin relation to the hill S_0. The growth process of the projection is considered as follows: first, a trigonal hill grows epitaxially on the substrate, then, a nucleation with a rotation-twin relation to the hill is formed on its side, from which a projection is developed. It is not probable that a projection grows to join a formerly developed trigonal hill from a nucleation formed separately on the substrate, because small and independent hills with the twin relation to the trigonal hill have never been found and growth toward the opposite to the tip of the projection is not easy. The reason why such a nucleation occurs at the side of the trigonal hill is not clear at present.

3.2.3. Rotation-twinned pyramid

Fig. 9 is a trigonal pyramid rarely grown on the surface of a trigonal hill. The growth direction of the pyramid is inclined to the normal of the hill surface by 39°.

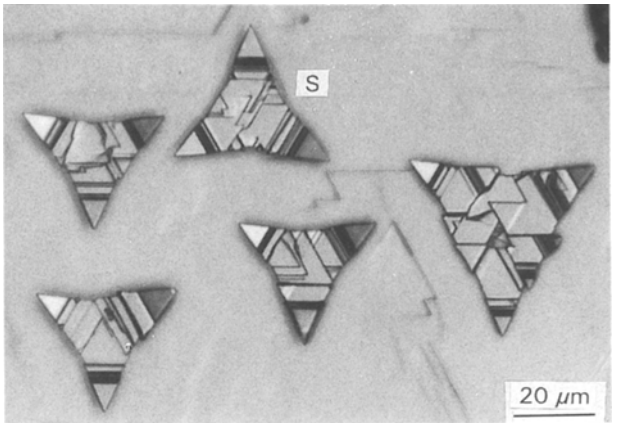

Figure 7 A trigonal hill S is in the opposite direction with respect to the other hills.

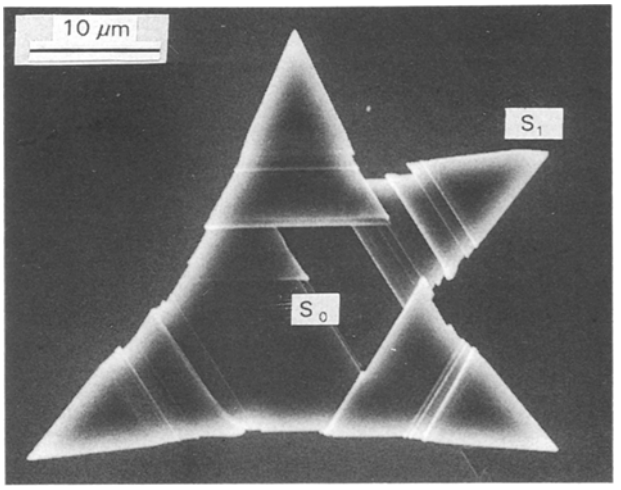

Figure 8 A trigonal hill S_1 is joined with a hill S_0 at its side. S_1 is in rotation-twin relationship to the thin ZnSe film, but S_0 is coherent to the film.

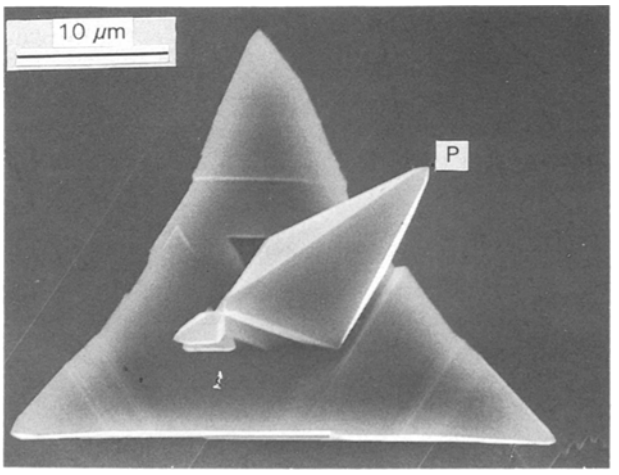

Figure 9 A trigonal pyramid P grown on the trigonal hill.

Fig. 10a and b show models of the tetrahedral bonding in the matrix and in the twinned crystal, respectively. White balls (A, A′) indicate Zn atoms and black balls (B, B′) Se atoms. In Fig. 10a, the bonds AB, BA′ and A′B′ are all in a $(0\,\bar{1}\,1)$, and the directions BA and B′A′ point the $[\bar{1}\,\bar{1}\,\bar{1}]$ B, along which the thin

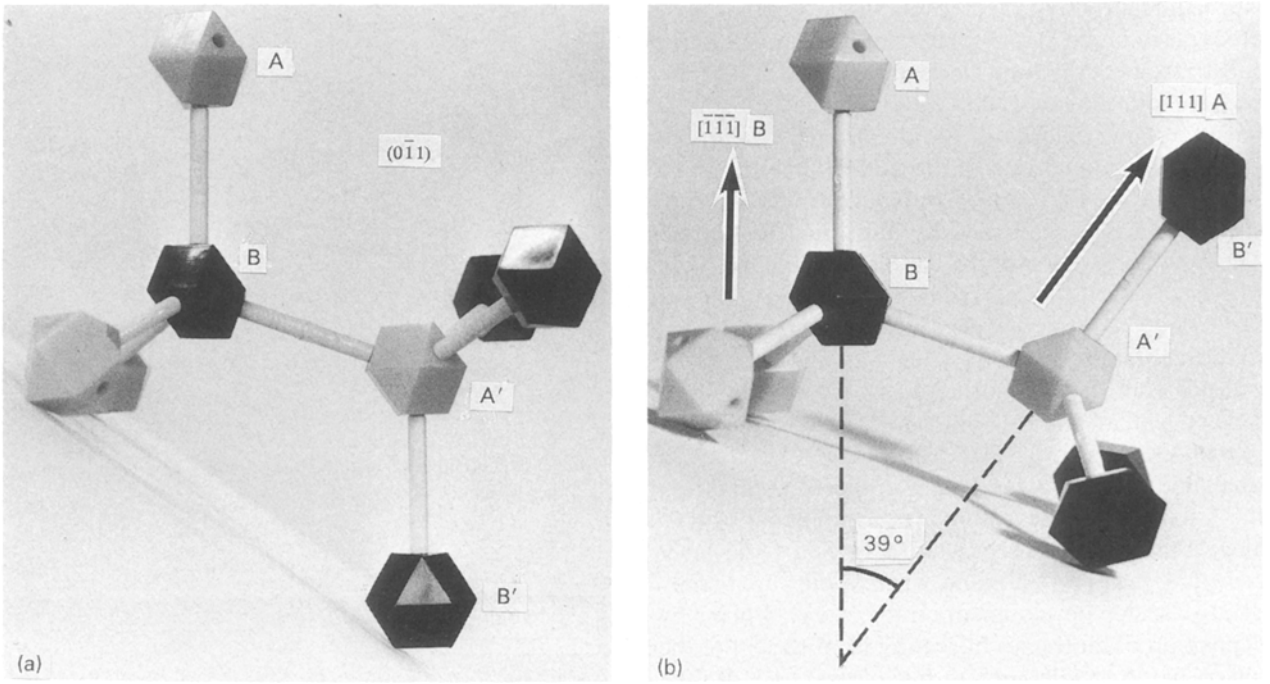

Figure 10 Models of tetrahedral bonding: (a) in the normal crystal, and (b) in the twinned crystal.

ZnSe film and the trigonal hill are grown. In Fig. 10b, the atomic configuration in the right-hand side of Fig. 10a is rotated by 60° or 180° around the axis A′B. The angle between the two directions BA and A′B′ is estimated to be 39°, which corresponds to the angle between the growth direction of the pyramid and the normal of the hill surface. Therefore, the pyramid grows along the [1 1 1] A; that is, a polar direction opposite to the one along which the trigonal hill and its tips grow, and it has a rotation-twin relation to the trigonal hill, rotated around the axis A′B (Fig. 10) by 60° or 180°.

The axis A′B is one of the polar axes ⟨1 1 1⟩ but is not parallel to the growth direction [$\bar{1}\,\bar{1}\,\bar{1}$] B of the trigonal hill. In this sense, the type of rotation twin found in the pyramid is different from the type found in the projection described in the previous section in which the rotation twin occurs around an axis parallel to the growth direction.

4. Conclusion

ZnSe crystals were epitaxially grown on the GaAs (1 1 1) A and ($\bar{1}\,\bar{1}\,\bar{1}$) B surfaces by the vapour transport method. Fine crystals and hexagonal plates were obtained on the (1 1 1) A surface of the substrate. Crystals obtained on the ($\bar{1}\,\bar{1}\,\bar{1}$) B, however, were uniform thin films 2 μm thick on which trigonal hills 5 μm thick were developed. Trigonal pyramids of 15 μm in height rarely grow on the surface of the trigonal hill. The trigonal hill and trigonal pyramid contained rotation twins around the polar axis parallel to the growth direction or around the other polar axis.

References

1. T. YAO, in "The Technology and physics of molecular beam epitaxy", edited by E. H. C. Parker (Plenum, New York, 1985) Ch. 10.
2. N. MATSUMURA, M. TSUBOKURA, J. SARAIE and Y. YODOGAWA, *J. Cryst. Growth* **86** (1988) 311.
3. A. YOSHIKAWA, S. YAMAGA, K. TANAKA and H. KASAI, *J. Cryst. Growth* **72** (1985) 13.
4. N. MATSUMURA, K. ISHIKAWA, J. SARAIE and Y. YODOGAWA, *J. Cryst. Growth* **72** (1985) 41.
5. H. MITSUHASHI, I. MITSUISHI and H. KUKIMOTO, *Japan. J. Appl. Phys.* **24** (1985) L864.
6. T. YAO and T. TAKEDA, *Appl. Phys. Lett* **48** (1986) 160.
7. M. KITAGAWA, A. SHINOHARA, J. SARAIE and T. TANAKA, *J. Cryst Growth* **63** (1983) 321.
8. K. MOCHIZUKI, K. MASUMOTO and H. IWANAGA, *J. Cryst Growth* **84** (1987) 1.
9. H. IWANAGA, N. SHIBATA and K. MOCHIZUKI, *J. Cryst Growth* **67** (1984) 97.
10. H. IWANAGA, T. YOSHIIE, S. TAKEUCHI and K. MOCHIZUKI, *J. Cryst Growth* **61** (1983) 691.
11. M. FUJII, H. IWANAGA and N. SHIBATA, *J. Cryst. Growth* **91** (1988) 229.

Received 2 March
and accepted 10 December 1992